Molecular Pharmacology Fast Forward. Published on September 25, 2019 as DOI: 10.1124/mol.119.115881
This article has not been copyedited and formatted. The final version may differ from this version.

Potential regulation of UGT2B10 and UGT2B7 by miR-485-5p in human liver

[a]Aimee K. Sutliff, [b]Jian Shi, [a]Christy J. W. Watson, [a]Martina Hunt, [a]Gang Chen, [b]Hao-Jie Zhu, and [a]Philip Lazarus

[a]Department of Pharmaceutical Sciences, Washington State University College of Pharmacy and Pharmaceutical Sciences, Spokane, WA (A.K.S., G.C., C.W., P.L.); [b]Department of Clinical Pharmacy, University of Michigan College of Pharmacy (J.S., H-J.Z.)

Molecular Pharmacology Fast Forward. Published on September 25, 2019 as DOI: 10.1124/mol.119.115881
This article has not been copyedited and formatted. The final version may differ from this version.

Running title: miR-485-5p regulation of UGT2B10 and UGT2B7

Corresponding author: Philip Lazarus, Ph.D., Department of Pharmaceutical Sciences, Washington State University College of Pharmacy and Pharmaceutical Sciences, PO Box 1495, Spokane, WA, 99210; Phone: 509-358-7947; Fax: 509-358-7967; Email: phil.lazarus@wsu.edu

Document Statistics:

Text pages: 24 (not including Abstract, Significance Statement, Acknowledgements, References, Figure Legends or Tables)

Tables: 1 (plus two Supplemental Tables)

Figures: 4

References: 40

Abstract words: 250

Introduction words: 600 (including citations)

Discussion words: 1485 (including citations)

Abbreviations: mass spectrometry (MS); microRNA (miRNA); messenger RNA (mRNA); quantitative reverse-transcription polymerase chain reaction (qRT-PCR); ribonucleic acid (RNA) single nucleotide polymorphism (SNP); site-directed mutagenesis (SDM); UDP-glucuronosyltransferase (UGT); untranslated region (UTR); uridine diphosphoglucuronic acid (UDPGA); indexed retention time (iRT)

Molecular Pharmacology Fast Forward. Published on September 25, 2019 as DOI: 10.1124/mol.119.115881
This article has not been copyedited and formatted. The final version may differ from this version.

Recommended section assignment: Metabolism, Transport, and Pharmacogenomics

Molecular Pharmacology Fast Forward. Published on September 25, 2019 as DOI: 10.1124/mol.119.115881
This article has not been copyedited and formatted. The final version may differ from this version.

Abstract

The UDP-glucuronosyltransferase (UGT) family of enzymes are important in the metabolic elimination of a variety of endogenous compounds such as bile acids, steroids, and fat-soluble vitamins, as well as exogenous compounds including many pharmaceuticals. The UGT2B subfamily are a major family of UGT enzymes expressed in human liver. The identification of novel mechanisms including post-transcriptional regulation by microRNA (miRNA) contribute to inter-individual variability in UGT2B expression and are crucial components in predicting patient drug response. In the present study, a high resolution liquid chromatography-tandem mass spectrometry (LC-MS/MS) method was employed to measure UGT2B protein levels in a panel of human liver microsomal samples (n=62). Concurrent *in silico* analysis identified eight candidate miRNA as potential regulators of UGT2B enzymes. Comparison of UGT2B protein expression and candidate miRNA levels from human liver samples demonstrated a significant inverse correlation between UGTs 2B10 and 2B15 and one of these candidate miRNAs, miR-485-5p. A near-significant correlation was also observed between UGT2B7 and miR-485-5p expression. *In vitro* analysis using luciferase-containing vectors suggested an interaction of miR-485-5p within the 3′ untranslated region (UTR) of UGT2B10. A significant reduction in luciferase activity was also observed for a luciferase vector containing the UGT2B7 3’ UTR; none was observed for the UBT2B15 3’-UTR. UGT2B10 and UGT2B7 activities were probed using nicotine and AZT, respectively, and significant decreases in glucuronidation activity were observed for both substrates in HuH-7 and Hep3B cells upon over-expression of miR-485-5p

Molecular Pharmacology Fast Forward. Published on September 25, 2019 as DOI: 10.1124/mol.119.115881
This article has not been copyedited and formatted. The final version may differ from this version.

mimic. This is the first study demonstrating a regulatory role for miR-485-5p for multiple UGT2B enzymes.

Molecular Pharmacology Fast Forward. Published on September 25, 2019 as DOI: 10.1124/mol.119.115881
This article has not been copyedited and formatted. The final version may differ from this version.

Significance Statement

The purpose of this study was to identify novel epigenetic microRNA regulators of the UDP-glucuronosyltransferase (UGT) 2B drug-metabolizing enzymes in healthy human liver samples. Our results indicate that microRNA 485-5p is a novel regulator of UGTs 2B7 and 2B10, which play an important role in the metabolism of many commonly prescribed medications, carcinogens and endogenous compounds. This study identified potential miRNA-UGT2B mRNA interactions using a novel proteomic approach, with in vitro experiments undertaken to validate these interactions.

Molecular Pharmacology Fast Forward. Published on September 25, 2019 as DOI: 10.1124/mol.119.115881
This article has not been copyedited and formatted. The final version may differ from this version.

Introduction

The UGT2B enzyme subfamily is involved in the metabolic clearance of numerous endogenous compounds including steroid hormones and bile acids, as well as exogenous agents including a variety of drugs and carcinogens (Stingl, Bartels, Viviani, Lehmann, & Brockmoller, 2014). UGT2B enzymes are well-expressed in the liver (Ohno & Nakajin, 2009) with it comprising approximately half of the hepatic UGT expression as determined in previous proteomic studies (Fallon, Neubert, Hyland, Goosen, & Smith, 2013).

The hepatically-expressed UGT2B isoforms include 2B4, 2B7, 2B10, 2B11, 2B15, and 2B17 (Jones & Lazarus, 2014; Mackenzie et al., 2005; Nakamura, Nakajima, Yamanaka, Fujiwara, & Yokoi, 2008; Ohno & Nakajin, 2009). Members of the UGT2B sub-family are comprised of six independent exons, exhibiting lower sequence homologies than either the 1A or 2A enzymes which exhibit an exon-sharing structure. UGT2Bs play an important role in drug metabolism and carcinogen detoxification. Therefore, identifying novel mechanisms involved in the regulation of UGT2B enzymes may provide insight into the mechanisms underlying overall metabolism in humans.

Recent studies have examined the role of microRNA (miRNA) in regulating UGT expression (Papageorgiou & Court, 2017; Tatsumi, Tokumitsu, Nakano, Fukami, & Nakajima, 2018; Wijayakumara, Mackenzie, McKinnon, Hu, & Meech, 2017). miRNA are short nucleotide fragments that bind in the 3' untranslated region (UTR) of mRNA and reduce translation of those transcripts, either by disruption of the mRNA structure through protein interactions which initiate deadenylation of the poly-A tail and uncapping

Molecular Pharmacology Fast Forward. Published on September 25, 2019 as DOI: 10.1124/mol.119.115881
This article has not been copyedited and formatted. The final version may differ from this version.

of the methylated 5' end (Fabian et al., 2011), or sequestration of the mRNA transcripts (Liu, Valencia-Sanchez, Hannon, & Parker, 2005). UGT1A gene expression has been shown to be regulated by miR-491-3p, with miR-491-3p expression levels inversely correlated with UGT1A3 and UGT1A6 mRNA levels in normal human liver, contributing to observed inter-individual variability in the expression of these enzymes (Dluzen et al., 2014). In addition, miR-376c exhibited an inverse expression pattern with the androgen-metabolizing UGTs 2B15 and 2B17 in prostate cancer cells (Wijayakumara, Hu, Meech, McKinnon, & Mackenzie, 2015). The opposite relationship between miR-376c and UGT2B15/UGT2B17 expression was shown in healthy prostate tissue, suggesting that low expression of miR-376c may contribute to prostate cancer development in androgen-dependent tumors by dysregulation of androgen signaling (Margaillan, Levesque, & Guillemette, 2016; Wijayakumara et al., 2015). miR-216b-5p was also shown to play a role in UGT2B regulation, with miR-216b-5p regulating UGTs 2B4, 2B7 and 2B10 in cell lines (Dluzen et al., 2016). A recent study identified miR-3664-3p as a potential regulator of UGT2B7 expression and activity (Wijayakumara et al., 2017), with an inverse correlation observed between UGT2B7 and miR-3664-3p expression in a panel of human tissues. Potential regulation of UGT2B4 by miR-135a-5p and miR-410-3p was also observed in the same study, with UGT2B4 expression reduced after miR-135a-3p and miR-410-3p over-expression, a pattern supported by a significant inverse expression correlation observed between UGT2B4 and miR-135a-5p as well as miR-410-3p in normal human tissues. In a screening of the 2,048 microRNA listed in miRbase version 19, Papageorgiou, et al. recently identified several microRNA that altered UGT2B7 and UGT2B15 activity *in vitro* (Papageorgiou & Court, 2017). Of these,

Molecular Pharmacology Fast Forward. Published on September 25, 2019 as DOI: 10.1124/mol.119.115881
This article has not been copyedited and formatted. The final version may differ from this version.

only the expression of miR-455-5p was shown to be correlated with altered UGT2B15 expression or glucuronidation activity in a panel of human livers; no miRNA were associated with altered UGT2B7 expression or activity in the same specimens.

In the present study, a proteomics approach was implemented to screen a panel of normal human liver specimens for miRNA potentially important in regulating UGT2B gene expression, with potential miRNA candidates examined for functionality *in vitro*. Results from the present study indicate that miRNA miR-485-5p may be a functional regulator of hepatic UGT2B10 and UGT2B7 expression.

Molecular Pharmacology Fast Forward. Published on September 25, 2019 as DOI: 10.1124/mol.119.115881
This article has not been copyedited and formatted. The final version may differ from this version.

Materials and methods

Chemicals and Reagents. The pGL3-Promoter luciferase and pRL-TK renilla plasmids as well as Dual-Luciferase Reporter Assay kits were obtained from Promega (Madison, WI). All synthesized DNA oligonucleotides used for 3' UTR amplification, site-directed mutagenesis (SDM), and PCR analysis were from Integrated DNA Technologies, Inc (Coralville, IA) or Life Technologies (Carlsbad, CA). Lipofectamine 3000 transfection reagent and Pierce BCA Protein Assay kits were from Life Technologies (Carlsbad, CA). Dulbecco's Modified Eagle's Medium (DMEM), penicillin-streptomycin (10,000 U/mL) and Opti-MEM Reduced Serum Media were purchased from Gibco (Carlsbad, CA) while fetal bovine serum (FBS) was purchased from VWR (Radnor, PA). Human liver microsomes (HLMs) were purchased from XenoTech, LLC (Kansas City, KS). miRVana miR-485-5p mimic (#MC10837), and miRVana negative control mimic #1 (#4464058) were purchased from Ambion/Thermo Fisher Scientific (Waltham, MA). qScript miRNA cDNA Synthesis Kit and PerfeCta SYBR Green SuperMix were purchased from Quanta Biosciences (Beverly, MA). Nicotine, uridine 5'-diphosphoglucuronic acid (UDPGA), alamethicin, trifluoroacetic acid, formic acid, and bovine serum albumin (BSA) were all purchased from Sigma-Aldrich (St. Louis, MO). 3'-Azido-3'-deoxythymidine (AZT), 3'-azido-3'-deoxythymidine-methyl-d_3-β-D-glucuronide (sodium salt; d3-AZT-glucuronide), 3'-azido-3'-deoxythymidine β-D-glucuronide (sodium salt; AZT-glucuronide), nicotine-β-D-glucuronide and nicotine-d_3-β-D-glucuronide were purchased from Toronto Research Chemicals (Toronto, Canada). Urea and dithiothreitol were purchased from Fisher Scientific (Pittsburgh, PA). Iodoacetamide and ammonium

Molecular Pharmacology Fast Forward. Published on September 25, 2019 as DOI: 10.1124/mol.119.115881
This article has not been copyedited and formatted. The final version may differ from this version.

bicarbonate were purchased from Acros Organics (Morris Plains, NJ), TPCK-treated trypsin was obtained from Worthington Biochemical Corporation (Freehold, NJ), and lysyl endopeptidase was purchased from Wako Chemicals (Richmond, VA). Water Oasis HLB columns were obtained from Waters Corporation (Milford, MA) while mass spectrometer-grade acetonitrile was purchased from (Avantor, Center Valley, PA). Indexed retention time (iRT) standard solutions were purchased from Biognosys AG (Cambridge, MA). All other chemicals were purchased from Fisher Scientific unless specified otherwise.

Cells and cell culture conditions. The human embryonic kidney 293 (HEK293) and human hepatocellular carcinoma Hep3B cell lines were purchased from the American Type Culture Collection (ATCC, Manassas, VA). The human hepatocellular carcinoma HuH-7 cell line was a kind gift from Dr. Jianming Hu (Penn State University, Hershey, PA). All cell lines were cultured in DMEM supplemented with 10% FBS and 1% penicillin/streptomycin, and grown and maintained in 5% CO_2 at 37°C.

Tissues. Liver specimens and corresponding total RNA (n=62) were obtained from the tissue bank at the H. Lee Moffitt Cancer Center Tissue Procurement Facility (Tampa, FL). All 62 subjects from whom liver specimens were obtained were Caucasian, with women comprising 44% (n=27) of these subjects. All specimens were obtained during resection for hepatocellular carcinoma and were deemed normal after pathology assessment, and were isolated and frozen at -70°C within 3 h post-surgery. All protocols involving the collection and analysis of tissue specimens from these tissue

Molecular Pharmacology Fast Forward. Published on September 25, 2019 as DOI: 10.1124/mol.119.115881
This article has not been copyedited and formatted. The final version may differ from this version.

banks were approved by their respective Institutional Review Boards and were in accordance with assurances filed with and approved by the United States Department of Health and Human Services.

miRNA binding site predictions. TargetScan is an *in silico* microRNA-mRNA binding prediction database that was used to generate a list of candidate microRNA. The criteria for selection of candidate microRNA included, (1) prediction to bind to individual UGT2B isoforms with a Context++ percentile above the 95th percentile within the TargetScan program, (2) prediction to bind to one of more other UGT2B isoforms, and (3) expression of candidate microRNA in human liver.

Real-Time Quantitative PCR. Total liver RNA concentrations were determined using a Nanodrop (ND-1000) spectrophotometer (Thermo Scientific), diluted and stored as aliquots in RNase-/DNAse-free water in a -80°C freezer. cDNAs were synthesized using the qScript miRNA cDNA Synthesis Kit. Real-time PCR was performed with PerfeCta SYBR Green SuperMix, cDNA corresponding to 50 ng of RNA, 100 nM of a universal reverse primer (provided by the PerfeCta kit), and 100 nM of the specific miRNA forward primer for either miR-135a-5p, miR-146a-3p, miR-196a-5p, miR-216a-5p, miR-216b-5p, miR-379-3p, miR-485-5p, miR-590-5p, miR-152-3p, or miR-23b-3p (Supplemental Table 1) as per the manufacturer's protocol. Reactions were performed in 15 µL total volume in 384-well plates using the BioRad CFX 384 real-time PCR machine, with incubations performed at 95°C for 2 min, followed by 40 cycles of 95°C for 10 sec, 60°C for 30 sec. Each plate included a no DNA negative control, and all

Molecular Pharmacology Fast Forward. Published on September 25, 2019 as DOI: 10.1124/mol.119.115881
This article has not been copyedited and formatted. The final version may differ from this version.

reactions were performed in quadruplicate. Expression analysis utilized the comparative C_T method and adapted using the method of Lamba et al. (Lamba, Ghodke-Puranik, Guan, & Lamba, 2014; Vandesompele et al., 2002). Briefly, the geometric mean of the expression of both miR152-3p and miR-23b-3p, which is the square root of the C_T value for miR-152-3p multiplied by the C_T value for miR-23b-3p, is used as a combined endogenous control for data normalization. miR152-3p and miR-23b-3p were used as controls since they were shown in previous studies to be more stable across human liver specimens than other controls (including U6 and RNU6B) in previous studies. The ΔC_T value for the candidate microRNA was calculated by subtracting the geometric mean of the combined controls from the C_T value. The $-\Delta Ct$ value was then used as the exponent to calculate the relative expression using a logarithm base 2, as is standard when using comparative analysis. C_T values were determined using the CFX Manager software (BioRad Laboratories).

All real-time values were normalized based on primer efficiencies. Briefly, each miRNA mimic was used as template in the qScript miRNA cDNA Synthesis reaction, as described above for the tissue samples. The resulting cDNA was diluted over a 5-log range and each dilution was used as template in quantitative PCR identical to those described above for the tissue samples. The C_T values for each dilution were plotted against the log of the dilution factor, and the slope of the regression line was calculated. The efficiency of each primer was calculated as E, where $E = 10^{-1/slope}$ (Pfaffl, 2004). Relative expression values for each miRNA in each tissue sample were calculated by first adjusting all C_T values for primer efficiency using $Log_2(E^{C_T})$, and then calculating relative expression using the standard $2^{\Delta Ct}$ method described by Pfaff et al.

Molecular Pharmacology Fast Forward. Published on September 25, 2019 as DOI: 10.1124/mol.119.115881
This article has not been copyedited and formatted. The final version may differ from this version.

Proteomics sample preparation. Human liver microsomal fractions were prepared from individual liver specimens as previously described (Coughtrie, Burchell, & Bend, 1986; Wiener, Fang, Dossett, & Lazarus, 2004). Protein concentration was measured using the Pierce BCA protein assay. Protein digestion was performed as previously described (Shi, Wang, Lyu, Jiang, & Zhu, 2018). Briefly, aliquots of 80 µg protein from liver microsomes were mixed with 0.2 µg of BSA internal standard. The protein mixture was precipitated with pre-cooled acetone and washed with 80% ethanol. Protein reduction was performed by adding 4 mM dithiothreitol in 8 M urea/100 mM ammonium bicarbonate at 37°C for 45 min, after which 20 mM iodoacetamide solution in 8 M urea/100 mM ammonium bicarbonate was added for alkylation at room temperature for 30 min in the dark. The urea concentration was adjusted to 6 M with 100 mM ammonium bicarbonate solution prior to digestion. Lysyl endopeptidase was added for the first digestion step at a protein to enzyme ratio of 100:1) at 37°C for 6 h. Samples were then diluted to 1.6 M urea with 50 mM ammonium bicarbonate, followed by a second digestion step with trypsin at a protein to enzyme ratio of 50:1 for an overnight incubation at 37°C. Digestion was terminated by adding 1 µL of trifluoroacetic acid. Digested protein peptides were extracted and purified using Waters Oasis HLB columns according to the manufacturer's instructions. Eluted peptides were dried in a SpeedVac SPD1010 concentrator and reconstituted in 80 µL of 3% acetonitrile containing 0.1% formic acid. The peptide samples were centrifuged and supplemented with synthetic iRT standard solutions prior to liquid chromatography-tandem mass spectrometry (LC-MS/MS) analysis.

Molecular Pharmacology Fast Forward. Published on September 25, 2019 as DOI: 10.1124/mol.119.115881
This article has not been copyedited and formatted. The final version may differ from this version.

LC-MS/MS-based protein quantification. Peptide samples were analyzed on a TripleTOF 5600+ mass spectrometer (AB Sciex, Framingham, MA) coupled with an Eksigent 2D plus LC system (Eksigent Technologies, Dublin, CA). LC separation was performed via a trap-elute configuration including a trapping column (ChromXP C18-CL, 120 Å, 5 µm, 0.3 mm cartridge, Eksigent Technologies, Dublin, CA) and an analytical column (ChromXP C18-CL, 120 Å, 150 x 0.3 mm, 5 µm, Eksigent Technologies, Dublin, CA). The mobile phase consisted of 0.1% formic acid in water (phase A) and 0.1% formic acid in acetonitrile (phase B). A total of 6 µg protein was injected for analysis. Peptides were trapped and cleaned on the trapping column with phase A delivered at a flow rate of 10 µL/min for 3 min before being separated on the analytical column with a gradient elution at a flow rate of 5 µL/min. The gradient time program was set as follows for phase B: 0 to 68 min: 3% to 30%, 68 to 73 min: 30% to 40%, 73 to 75 min: 40% to 80%, 75 to 78 min: 80%, 78 to 79 min: 80% to 3%, and finally 79 to 90 min at 3% for column equilibration. The TripleTOF instrument was operated in a positive ion mode with an ion spray voltage floating at 5500 v, ion source gas one at 28 psi, ion source gas two at 16 psi, curtain gas at 25 psi, and source temperature at 280°C.

To generate the reference spectral library, Information-Dependent Acquisition (IDA) was performed on three pooled human liver microsomal samples. The IDA method was set up with a 250 ms TOF-MS scan from 400 to 1250 Da, followed by an MS/MS scan in high sensitivity mode from 100 to 1500 Da (50 ms accumulation time, 10 ppm mass tolerance, charge state from +2 to +5, rolling collision energy and dynamic accumulation) of the top 30 precursor ions from the TOF-MS scan. The IDA

Molecular Pharmacology Fast Forward. Published on September 25, 2019 as DOI: 10.1124/mol.119.115881
This article has not been copyedited and formatted. The final version may differ from this version.

data from the pooled liver microsomes were searched by MaxQuant (version 1.5.3.30, Max Planck Institute of Biochemistry, Germany). The human proteome fasta file with 20,237 protein entries downloaded from Uniport on 3/2/2017 was used as the reference sequences for the search. Trypsin/P was used as the protease. Peptide length was between 7 and 25 residues with up to two missed cleavage sites allowed. Carbamidomethyl (C) was set as a fixed modification. A false discovery rate of 0.01 was used as the cutoff for both peptide and protein identification.

All liver microsomal samples were analyzed using a sequential window acquisition of all theoretical mass spectra (SWATH) method comprised of a 250 ms TOF-MS scan from 400 to 1250 Da, followed by MS/MS scans from 100 to 1500 Da performed on all precursors in a cyclic manner. The isolation scheme was set as “SWATH (VW 100)”. The accumulation time was 50 ms per isolation window, resulting in a total cycle time of 2.8 s. The spectral alignment and target data extraction of the SWATH data were performed on Skyline-daily (version 3.7.1.11271, University of Washington, Seattle, WA) with the reference spectral library generated from the IDA searches. The MS1 and MS/MS filtering were both set as “TOF mass analyzer” with the resolution power of 30,000 and 15,000, respectively. The retention time prediction was based on the auto-calculate regression implemented in the iRT calculator. Proper peak selection was checked manually with the automated assistance of Skyline-daily. The surrogate peptides used for the quantification of UGT2B4, 2B7, 2B10, 2B15, 2B17 and BSA are listed in Supplemental Table 2. These peptides were selected based on the uniqueness and chromatographic performance. The peak areas of the top 3 to 5

Molecular Pharmacology Fast Forward. Published on September 25, 2019 as DOI: 10.1124/mol.119.115881
This article has not been copyedited and formatted. The final version may differ from this version.

fragment ions were summed up and normalized to the internal standard BSA for quantification.

Construction of reporter plasmids. The 3' UTR of UGTs 2B7, 2B10 and 2B15 were inserted into the *XbaI* restriction enzyme site lying 3' of and adjacent to the luciferase gene within the pGL3-Promotor vector (Promega; Madison, WI) to simulate the sequence position in the native UGT2B mRNA transcript. In order to include the entire 3' UTR sequence, primers were designed to amplify the full 3' UTR of UGT2B10 (1138 nt) and UGT2B15 (467 nt), flanked by the TCTAGA *XbaI* restriction sequence plus an additional four nt to ensure the restriction site nucleotides are not lost during PCR amplification (Supplementary Table 1). The luciferase-containing plasmid used for analysis of the UGT2B7 3' UTR (251 nt) was created and described for a previous study (Dluzen et al., 2016).

To identify the miR-485-5p-binding site within the 3' UTR of UGT2B10, four nucleotides within the miRNA recognition element (MRE, see Figure 1) identified by TargetScan were removed by site directed mutagenesis, following the manufacturer's protocols. To identify the miR-485-5p-binding site within the 3' UTR of UGT2B7, two sites were similarly mutated by deleting four nucleotides in two potential miRNA recognition elements within the 3'UTR of UGT2B7 (Figure 1). The first site was selected based on its similarity to the predicted binding site of UGT2B10, with the exception of two uracils in the potential UGT2B7 MRE in place of two cytosines in the UGT2B10 MRE. The second site was selected due to the presence of five nucleotides with a Watson-Crick binding pair and a guanine-uracil wobble pair in the second nucleotide of

Molecular Pharmacology Fast Forward. Published on September 25, 2019 as DOI: 10.1124/mol.119.115881
This article has not been copyedited and formatted. The final version may differ from this version.

the miRNA seed sequence. These potential binding sites are located 35-55 (termed 'Site 1') and 230-251 (termed Site 2) nucleotides downstream of the UGT2B7 translational stop codon. Verification of the manually-identified MRE's within the UGT2B7 3' UTR was accomplished by removal of those predicted binding sites. Using the pGL3-UGT2B7 3'UTR plasmid as template, four nucleotides in each potential MRE were deleted using the mutagenesis primers listed in Supplemental Table 1. All sequences used in this study were confirmed by Sanger sequencing analysis carried out by Genewiz (Plainfield, NJ).

Luciferase assays. HEK293 cells were seeded onto 12-well plates at 50,000 cells/well. After 24 h, cells were co-transfected with 380 ng of UGT2B 3' UTR-containing pGL3 luciferase plasmid, 20 ng of the pRL-TK control vector and either 100 nM scrambled miRNA control or 100 nM miR-485-5p mimic. For each well, 2 µL of Lipofectamine 3000 transfection reagent was added to the plasmids and miRNA mimics in Opti-MEM and incubated for 15 min according to the manufacturer's protocol. Whole cell homogenates were lysed 24 h post-transfection using the passive lysis buffer provided with the Dual-Luciferase Reporter Assay kit. Firefly and renilla luciferase activity was measured separately upon addition of Luciferase Assay Reagent II and Stop & Glo reagent, respectively, with a luminometer (Bio-tek Synergy HT, Winooski, VT). All luciferase assay experiments were performed in triplicate, with each experimental and control group the result of triplicate treatments.

Molecular Pharmacology Fast Forward. Published on September 25, 2019 as DOI: 10.1124/mol.119.115881
This article has not been copyedited and formatted. The final version may differ from this version.

Glucuronidation Assays. HuH-7 or Hep3B cells were transfected with either 100 nM scrambled miRNA controls or miR-485-5p mimic using 8 uL of Lipofectamine 3000 in 10 cm dishes, according to the manufacturer's protocol. Cells were collected 48 h post transfection. Cell pellets underwent five freeze-thaw cycles and were homogenized by passing them through a 27 gauge needle ten times prior to storage at -80°C. Protein concentration was determined using the BCA Protein Assay Kit (Pierce Chemical, Rockford, IL) and measured using the Synergy Neo and Gen5 Data Analysis Software (BioTek, Winooski, VT).

Glucuronidation assays included HuH-7 or Hep3B cell homogenate (50 µg), substrate, 50 mM Tris-HCl (pH 7.4), 10 mM $MgCl_2$ and 4 mM UDPGA, and were performed at 37°C. For UGT2B7 activity assessment, cell homogenate was incubated with 5 mM AZT for 60 min; for UGT2B10, cell homogenate was incubated with 500 µM nicotine for 2 h (Chen, Blevins-Primeau, Dellinger, Muscat, & Lazarus, 2007; Walsky et al., 2012). Incubation times were confirmed to be within the linear phase as determined in time-course experiments. Glucuronidation reactions were spiked with either d3-AZT-glucuronide for UGT2B7 or d3-nicotine-glucuronide for UGT2B10, and terminated by adding an equal volume of cold 100% acetonitrile. Reactions were centrifuged for 10 min at 16,000 g and supernatant was collected for analysis on LC-MS/MS. Human liver microsomes (HLM) were used as a positive control, with d3-labeled standards spiked into each sample to confirm peak identity. As a negative control, assays containing HLMs assays were performed without UDP-glucuronic acid. Glucuronide metabolites were analyzed on a Sciex QTRAP 6500 LC-MS/MS System (Framingham, MA), using the specific conditions listed below. Quantification was based on multiple independent

Molecular Pharmacology Fast Forward. Published on September 25, 2019 as DOI: 10.1124/mol.119.115881
This article has not been copyedited and formatted. The final version may differ from this version.

assays utilizing internal standards and validated standard curves of the glucuronide metabolites, using Sciex MultiQuant 2.1 software. A minimum of 4 experiments were performed for each assay.

AZT-glucuronide formation was analyzed using a 1.7 µ ACQUITY UPLC BEH C18 analytical column (2.1 mm x 50 mm, Waters Milford, MA) in series with a 0.2 µm Waters assay frit filter (2.1 mm). Gradient elution was performed with a flow rate of 0.4 mL/min, starting with 95% Buffer A (5 mM ammonium acetate 0.1% formic acid) and 5% Buffer B (100% acetonitrile) for 30 sec, a subsequent linear gradient to 50% Buffer B over 2.5 min, and then 95% Buffer B maintained over the next 2 min for re-equilibration. AZT-glucuronide and d3-AZT-glucuronide was monitored using multiple reaction monitoring (MRM) with transitions *m/z* 442.000 →125.100 for AZT-glucuronide and *m/z* 445.000 to 128.100 for d3-AZT-glucuronide. Identification of AZT-glucuronide was confirmed using an AZT-glucuronide standard.

Nicotine glucuronides were analyzed using a Waters ACQUITY UPLC BEH HILIC 1.7 µm analytic column (2.1 x 100 mm). Gradient conditions were performed with a 0.4 mL/min flow rate, starting with 80% Buffer B (5 mM NH_4Ac in 90% acetonitrile) for 1 min and 50 sec, followed by a steep gradient to 100% Buffer A (5 mM NH_4Ac in 60% acetonitrile) for 3 min, and then back to 80% Buffer B for the remainder of the 10 min run. Nicotine-glucuronide was determined using MRM, with mass transitions of *m/z* 339.1 → 163.1 for nicotine-glucuronide, and an *m/z* 163.1 → 106.0 for d3-nicotine glucuronide.

Molecular Pharmacology Fast Forward. Published on September 25, 2019 as DOI: 10.1124/mol.119.115881
This article has not been copyedited and formatted. The final version may differ from this version.

Statistical Analysis. The entire set (n=62) of liver specimens available to the investigators were used for the liver proteomics analysis; an initial power calculation was not performed *a priori*. Statistical analysis was performed using Graphpad Prism 5 software (La Jolla, CA). For all studies examining the effects of over-expressed miR-485-5p miRNA mimic, the one-tailed Student's t-test was performed. The correlation between of UGT2B protein levels to and miRNA expression were described by the Pearson correlation coefficient with a one-tailed p-value. Error bars presented in Figures 3 and 4 were standard deviation (S.D.).

Molecular Pharmacology Fast Forward. Published on September 25, 2019 as DOI: 10.1124/mol.119.115881
This article has not been copyedited and formatted. The final version may differ from this version.

Results

miRNA predicted to bind to UGT2B mRNA were identified using TargetScan. Candidate miRNAs were selected if the TargetScan context score was in the 95th percentile for at least one of the UGT2Bs and the miRNA was predicted to bind to at least one other 2B member. While miR-485-5p was only predicted to bind to a single UGT2B (UGT2B10), it was included in the current study because only miR135a-5p exhibited a higher score profile (including context++ score and conserved branch length). The final miRNA candidates (with their predicted targeted UGT2Bs in parenthesis) were: miR-379-5p (UGT2B4 and UGT2B10), miR-135a-5p (UGTs 2B4, 2B10, 2B15, and 2B17), miR-590-5p (UGTs 2B4, 2B15 and 2B17), miR-216a-5p (UGTs 2B7 and 2B10), miR-216b-5p (UGTs 2B4, 2B7 and 2B10), miR-146a-3p (UGTs 2B7 and 2B10), miR-485-5p (UGT2B10), and miR-196a-5p (UGTs 2B4 and 2B7).

The expression of candidate miRNA was examined by real-time PCR using total RNA from a panel of 62 individual normal human liver specimens. All candidate miRNA amplified successfully, with miR-590-5p exhibiting the highest expression, followed by miR-379-5p and miR-216b-5p (Table 1). miR-485-5p was the least expressed miRNA, but it was expressed with a C_T value of less than 29 for all 62 liver specimens examined.

The relative abundance of each of the UGT2B enzymes within the same panel of human liver specimens was determined by LC-MS/MS SWATH analysis. Pearson correlation analysis was performed to test if miRNAs levels were negatively associated with individual UGT protein levels. A significant inverse correlation was observed

Molecular Pharmacology Fast Forward. Published on September 25, 2019 as DOI: 10.1124/mol.119.115881
This article has not been copyedited and formatted. The final version may differ from this version.

between the expression of both UGT2B10 (P=0.047, r=-0.214) and UGT2B15 (P=0.038, r=-0.228), and the expression of miR-485-5p in the 62 human liver specimens (Figure 2). A trend towards an inverse correlation was also observed for miR-485-5p and the expression of UGT2B7 (P=0.096, r=-0.167). For both UGT2B4 and UGT2B17, there were no significant association with the expression of any of the tested miRNA candidates in the 62 human liver specimens examined in this study. For UGT2B17, five samples were removed from the data set since they were previously shown to be from individuals homozygous for a known UGT2B17 whole-gene deletion polymorphism (Gallagher et al., 2007), and therefore exhibited no UGT2B17 expression regardless of miRNA levels. None of the other miRNA tested exhibited a significant correlation (i.e., with a $P<0.05$) between the expression of any of the UGT2B enzymes and any of the other seven miRNA tested.

To test if overexpressed miR-485-5p negatively regulated the expression of UGT2B enzymes, the 3' UTRs of UGTs 2B7, 2B10 and 2B15 were cloned downstream of the luciferase gene within the pGL-3 reporter vector. Each vector was co-transfected with TK-Renilla transfection control plasmid and either 100 nM scrambled miRNA control or miR-485-5p mimic. A significant (*P*=0.022) 29% decrease in luciferase activity was observed after co-transfection of 100 nM miR-485-5p mimic with the wt UGT2B10 3'-UTR-containing pGL-3 vector in HEK293 cells (Figure 3, panel A). When comparing cells transfected with the UGT2B10 3' UTR seed deletion mutant plasmid, there was a near-identical level of luciferase activity observed for cells co-transfected with miR-485-5p as compared to cells co-transfected with the scrambled mimic control miRNA. A significant (*P*=0.0060) 55% decrease in luciferase activity was observed for cells co-

Molecular Pharmacology Fast Forward. Published on September 25, 2019 as DOI: 10.1124/mol.119.115881
This article has not been copyedited and formatted. The final version may differ from this version.

transfected with 100 nM of miR-485-5p mimic together with the pGL-3 vector containing the UGT2B7 3′ UTR (Figure 3, Panel B). No effect on luciferase activity was observed for cells co-transfected with 100 nM of miR-485-5p mimic and the pGL-3 vector containing the UGT2B15 3’ UTR (Figure 2, Panel C).

In silico analysis of 3’ UTR sequences by TargetScan only predicted an MRE site in UGT2B10. However, proteomic and luciferase assay data suggested that miR-485-5p also potentially interacts with the 3’ UTR of UGT2B7. To identify the mRNA sequence that miR-485-5p may be binding to in the UGT2B7 3’ UTR sequence, two potential miR-485-5p MREs were manually-identified within the UGT2B7 3’ UTR, and each was mutated individually to remove four nucleotides from their seed sequence. For Site 1, nucleotides corresponding 45-48 downstream of the stop codon were deleted, while nucleotides corresponding to 245-248 downstream of the stop codon were deleted for Site 2 (see Figure 1). A third plasmid was also created with both sites mutated. As shown in Figure 3 (panel B), similar levels of inhibition of luciferase activity were observed in cells transfected with any of the three UGT2B7 3’-UTR-mutated luciferase plasmids when cells were co-transfected with miR-485-5p mimic vs. scrambled mimic. These data suggest that neither of the manually predicted sites were acting as MREs for miR-485-5p within the UGT2B7 3’-UTR.

In previous studies, several UGT2B enzymes including UGTs 2B10 and 2B7 were shown to be expressed in both the HuH-7 and Hep3B cells lines (Dluzen et al., 2016). The expression of these UGTs in these cell lines was confirmed in the present study, with UGT2B7 demonstrating between 5-20-fold higher levels of expression than UGT2B10 in the two lines (results not shown). These cell lines also exhibit endogenous

Molecular Pharmacology Fast Forward. Published on September 25, 2019 as DOI: 10.1124/mol.119.115881
This article has not been copyedited and formatted. The final version may differ from this version.

expression of miR-485-5p (Zhang, Zhou, & Lu, 2018), making them excellent cell line models to examine the potential regulation of 2B enzymes by miR-485-5p. The expression of miR-485-5p in both cell lines was confirmed in the present study, with it expressed at levels that were ~1.8-fold higher in Hep3B cells as compared to HuH-7 cells (results not shown). HuH-7 and Hep3B cells were transfected with miR-485-5p mimic and *in vitro* glucuronidation assays were performed using homogenate from miRNA-transfected cells and either the UGT2B10-specific substrate, nicotine, or the UGT2B7-specific substrate, AZT. Significant decreases in nicotine-glucuronide formation of 52% and 44% were observed in HuH-7 (P=0.0003) and Hep3B (P=0.016) cell homogenates, respectively, after over-expression of 100 nM miR-485-5p mimic in assays containing 500 µM nicotine (Figure 4, panel A). Similarly, significant decreases of 27% (P=0.017) and 31% (P=0.030) in AZT-glucuronide formation were observed in HuH-7 and Hep3B, respectively, after transfection with 100 nM miR-485-5p (Figure 4, panel B).

Molecular Pharmacology Fast Forward. Published on September 25, 2019 as DOI: 10.1124/mol.119.115881
This article has not been copyedited and formatted. The final version may differ from this version.

Discussion

The exploration of potential miRNA regulators of metabolizing enzymes may provide insight into the variability of an individual's ability to detoxify UGT2B specific substrates. Using a proteomic approach, the current study examined the expression of five hepatic UGT2B enzymes and eight miRNA predicted *in silico* to bind to UGT2B 3' UTR sequences in 62 normal human liver samples. While UGTs 2B10 and 2B15 were the only UGT2B enzyme to exhibit statistically significant inverse expression relationship with one of the miRNA candidates examined in this study (miR-485-5p), UGT2B7 showed a similar but non-significant inverse relationships with the same miRNA, indicating the potential for downregulation of multiple UGT2B family members by miR-485-5p. An effect by miR-485-5p on the expression of both UGTs 2B10 and 2B7 was confirmed in assays with a luciferase vector containing the 3' UTRs of either UGT2B10 or UGT2B7; a similar effect was not observed for UGT2B15. This effect was further validated in two different cell lines, with over-expression of the miR-485-5p mimic resulting in significantly decreased UGT2B10 and UGT2B7 activities against known specific substrates in HuH7 and Hep3B cell homogenates. These data strongly suggest that miR-485-5p plays an important role in regulating the expression of these two UGT enzymes. In addition, the current study measured UGT2B protein levels in a panel of liver specimens by SWATH-MS analysis, with expression levels of candidate miRNA quantified by qPCR in the same specimens. The ability to measure total protein levels in biological samples using this technique can provide a highly sensitive and reproducible

Molecular Pharmacology Fast Forward. Published on September 25, 2019 as DOI: 10.1124/mol.119.115881
This article has not been copyedited and formatted. The final version may differ from this version.

tool (Collins et al., 2017) to be applied to the study of miRNA regulation in specific tissues.

UGT2B10 is a key enzyme involved in the N-glucuronidation of many drugs that contain an amine group (Lu, Xie, & Wu, 2017), including the antipsychotics loxapine, clozapine and chlorpromazine, as well as the tricyclic amine drugs amitriptyline and imipramine (Kato et al., 2013). A diminished ability to detoxify these drugs could lead to liver toxicity in individuals with low expression of UGT2B10. In addition, UGT2B10 is the major UGT responsible for the clearance of nicotine and its major metabolite, cotinine (Chen et al., 2007), and is important in the metabolism and detoxification of tobacco-specific nitrosamines (TSNAs) present in tobacco and smokeless tobacco products (Chen, Dellinger, Sun, Spratt, & Lazarus, 2008). Therefore, downregulation of UGT2B10 by miRNA including miR-485-5p could potentially lead to higher levels of exposure to nicotine or TSNAs, which could affect nicotine addiction and susceptibility to the carcinogenic effects of TSNAs.

In silico analysis predicted a miR-485-5p/UGT2B10 3'-UTR MRE located at 280-300 bp 3' of the translation stop codon, and deletion analysis of this MRE site demonstrated a specific effect by overexpression of the miR-485-5p mimic. The UGT2B7 3′ UTR contains no predicted miR-485-5p miRNA recognition element (MRE) within its 3′ UTR based on an *in silico* screening using TargetScan. However, the predicted MRE in the UGT2B10 3' UTR is similar to a region in the UGT2B7 3' UTR located 35 nucleotides downstream of the UGT2B7 translational stop codon (Site 1; see Figure 1). This proposed UGT2B7 MRE contains two uracils in place of two cytosines within the UGT2B10 MRE, and one less binding pair at the 3' UTR end of this potential

Molecular Pharmacology Fast Forward. Published on September 25, 2019 as DOI: 10.1124/mol.119.115881
This article has not been copyedited and formatted. The final version may differ from this version.

UGT2B7 MRE. The GU wobble in RNA may account for predictions that include guanine and uracil pairs in place of Watson and Crick binding partners. Another possible site (Site 2) for binding within the 3' UTR of UGT2B7 is located 230 nucleotides downstream of its translational stop codon. This site shares only six nucleotides with the predicted UGT2B10 MRE, with one GU pair wobble pair and an additional A in the flanking 3' end of the UGT2B7 mRNA sequence. Interestingly, deletion of these sites within the UGT2B7 3' UTR of the pGL3 vector resulted in no diminished effect by miR-485-5p mimic overexpression on luciferase activity, suggesting that neither of these sites act as a functional MRE within the UGT2B7 3'-UTR for miR-485-5p.

The other members of the UGT2B family in this study did not show any significant associations between hepatic UGT2B protein and expression of the miRNAs examined. Although there were no predicted binding sites within the 3' UTR of UGT2B15 for miR-485-5p, luciferase assays were performed for this gene due to a significant inverse expression relationship observed between miR-485-5p and UGT2B15 expression in the panel of liver specimens examined in this study. In addition, the UGT2B15 3' UTR sequence contains a possible MRE located 132 nucleotides downstream of the UGT2B15 stop codon, where the eight nucleotide binding pairs on the 3' end of the miRNA includes two GU wobble pairs. However, unlike that observed for UGTs 2B10 and 2B7, no effect on luciferase activity was observed for *in vitro* assays using a luciferase vector containing the UGT2B15 3' UTR.

Several of the miRNA selected as candidates for this study were predicted to bind to multiple UGT2B isoforms. While enzymes within the UGT1A and UGT2A (excluding UGT2A3) sub-families share the same 3' UTR, the UGT2B genes are

Molecular Pharmacology Fast Forward. Published on September 25, 2019 as DOI: 10.1124/mol.119.115881
This article has not been copyedited and formatted. The final version may differ from this version.

independent of each other, exhibiting no exon sharing. However, there is relatively high homology between 3' UTRs for several of the UGT2B genes. While the 3' UTR for UGT2B7 is only roughly one-third the length that of UGT2B10, this sequence exhibits over 80% homology to comparable sequences within UGT2B10 as determined using the ExPASy Bioinformatics Resource Portal SIM alignment tool (https://www.expasy.org). Yet, only miR-485-5p demonstrated a significant association with UGT2B expression, and only for UGTs 2B10 and 2B7. Previous studies identified miR-491-3p as a candidate to bind to the 3' UTR of all UGT1A isoforms, which contain the same 3' UTR (Dluzen et al., 2014). miR-491-3p was shown to regulate the expression of UGTs 1A1, 1A3 and 1A6, but not UGTs 1A4 or 1A9, and significant inverse associations were found in human liver specimens between miR-491-3p and the expression of both UGTs 1A3 and 1A6 but not UGT1A1. It was suggested that differences in secondary structure could be responsible for this differential regulation (Dluzen et al., 2014). A similar mechanism could also be playing a role in the differential regulation of UGT2B enzymes.

miR-485-5p has been shown to be involved in the regulation of a number of other cellular pathways. The long non-coding RNA, NEAT1, was found to reduce the levels of miR-485-5p expression, and a corresponding increase in STAT3 expression was observed in both HuH-7 and Hep3B cells (Zhang et al., 2018). When STAT3 is repressed, hepatocellular carcinoma (HCC) cell migration and invasion is reduced and low levels of miR-485-5p are associated with increased HCC cancer metastasis (Zhang et al., 2018). miR-485-5p has also been linked to liver cancer by targeting the extracellular matrix metalloproteinase inducer (EMMPRIN). Reduced miR-485-5p

Molecular Pharmacology Fast Forward. Published on September 25, 2019 as DOI: 10.1124/mol.119.115881
This article has not been copyedited and formatted. The final version may differ from this version.

expression and associated increases in EMMPRIN expression were correlated with increased HCC tumor progression and metastasis (Sun, Liu, Li, Wang, & Wang, 2015). A similar association between low miR-485-5p expression and HCC tumor progression and metastasis was observed in studies by Guo et al. (Guo, Li, Ma, Shi, & Ren, 2015), with stanniocalcin 2 identified as a potential miR-485-5p target. Other studies have implicated miR-485-5p regulation of several tumor suppressor genes, with high miR-485-5p expression associated with greater tumor suppression and better patient prognosis (Huang et al., 2018; Kang, Ren, Zhao, Li, & Deng, 2015; Lou et al., 2016). Results of the present study demonstrate an effect by miR-485-5p on UGT2B10 and UGT2B7 expression and suggest that variations in miR-485-5p expression could also play an important role in liver toxicity in patients treated with drugs metabolized by these two enzymes, including epirubicin, zidovudine, and codeine (Court et al., 2003; Innocenti, Iyer, Ramirez, Green, & Ratain, 2001), and loxapine, amitriptyline, and chlorpromazine (Lu et al., 2017), for UGT2B7 and UGT2B10, respectively.

Previous *in vitro* studies had implicated miR-216b-5p in the regulation of several UGT2B enzymes (Dluzen et al., 2016). While the expression of miR-216b-5p was shown to be expressed in pooled liver RNA, an analysis of miR-216b vs. UGT2B expression was not performed in human tissues in that study. Interestingly, a significant inverse relationship between the expression of miR-216b-5p and UGT2B enzymes was not observed in the 62 liver specimens examined in the present study. Potentially, differences in the expression of miR-216b-5p in hepatic tissue vs. cell lines could help explain this discrepancy. miR-216b-5p was shown to be expressed up to 900-lower in liver than in some other human tissues including pancreas (Dluzen et al., 2016).

Molecular Pharmacology Fast Forward. Published on September 25, 2019 as DOI: 10.1124/mol.119.115881
This article has not been copyedited and formatted. The final version may differ from this version.

Interestingly, over-expression of UGTs 2B4, 2B7 and 2B15 reduced lipid accumulation in the Panc-1 pancreatic cell line (Dates et al., 2015). Excess lipid levels in cancer cells are known to contribute to proliferation in pancreatic cells (Beloribi-Djefaflia, Vasseur, & Guillaumond, 2016), suggesting that it is possible that miR-216b-5p is playing a far more critical role in regulating the expression of UGT2Bs in the pancreas than in the liver.

In summary, the present study suggests that miR-485-5p exhibits a regulatory role for UGT2B10 and UGT2B7. This regulation could impact liver toxicity in response to doses considered safe for a number of the top over-the-counter and prescription drugs.

Molecular Pharmacology Fast Forward. Published on September 25, 2019 as DOI: 10.1124/mol.119.115881
This article has not been copyedited and formatted. The final version may differ from this version.

Acknowledgments

The authors thank the Mass Spectrometry Core facility at Washington State University Spokane for their help with LC/MS.

Molecular Pharmacology Fast Forward. Published on September 25, 2019 as DOI: 10.1124/mol.119.115881
This article has not been copyedited and formatted. The final version may differ from this version.

Authorship Contributions

Participated in research design: Sutliff, Shi, Hunt, Watson, Chen, Zhu, Lazarus

Conducted experiments: Sutliff, Shi, Hunt

Contributed new reagents or analytic tools: Sutliff, Shi, Watson, Chen, Zhu, Lazarus

Performed data analysis: Sutliff, Shi, Hunt, Watson, Chen, Zhu, Lazarus

Wrote or contributed to writing of the manuscript: Sutliff, Shi, Watson, Chen, Zhu, Lazarus

References

Beloribi-Djefaflia, S., Vasseur, S., & Guillaumond, F. (2016). Lipid metabolic reprogramming in cancer cells. *Oncogenesis, 5*, e189. doi:10.1038/oncsis.2015.49

Chen, G., Blevins-Primeau, A. S., Dellinger, R. W., Muscat, J. E., & Lazarus, P. (2007). Glucuronidation of nicotine and cotinine by UGT2B10: loss of function by the UGT2B10 Codon 67 (Asp>Tyr) polymorphism. *Cancer Res, 67*(19), 9024-9029. doi:67/19/9024 [pii]

10.1158/0008-5472.CAN-07-2245

Chen, G., Dellinger, R. W., Sun, D., Spratt, T. E., & Lazarus, P. (2008). Glucuronidation of tobacco-specific nitrosamines by UGT2B10. *Drug Metab Dispos, 36*(5), 824-830. doi:dmd.107.019406 [pii]

10.1124/dmd.107.019406

Collins, B. C., Hunter, C. L., Liu, Y., Schilling, B., Rosenberger, G., Bader, S. L., . . . Aebersold, R. (2017). Multi-laboratory assessment of reproducibility, qualitative and quantitative performance of SWATH-mass spectrometry. *Nat Commun, 8*(1), 291. doi:10.1038/s41467-017-00249-5

Coughtrie, M. W., Burchell, B., & Bend, J. R. (1986). A general assay for UDPglucuronosyltransferase activity using polar amino-cyano stationary phase HPLC and UDP[U-14C]glucuronic acid. *Anal Biochem, 159*(1), 198-205.

Court, M. H., Krishnaswamy, S., Hao, Q., Duan, S. X., Patten, C. J., Von Moltke, L. L., & Greenblatt, D. J. (2003). Evaluation of 3'-azido-3'-deoxythymidine, morphine, and codeine as probe substrates for UDP-glucuronosyltransferase 2B7 (UGT2B7) in human liver microsomes: specificity and influence of the UGT2B7*2 polymorphism. *Drug Metab Dispos, 31*(9), 1125-1133. doi:10.1124/dmd.31.9.1125

Dates, C. R., Fahmi, T., Pyrek, S. J., Yao-Borengasser, A., Borowa-Mazgaj, B., Bratton, S. M., . . . Radominska-Pandya, A. (2015). Human UDP-Glucuronosyltransferases: Effects of altered expression in breast and pancreatic cancer cell lines. *Cancer Biol Ther, 16*(5), 714-723. doi:10.1080/15384047.2015.1026480

Dluzen, D. F., Sun, D., Salzberg, A. C., Jones, N., Bushey, R. T., Robertson, G. P., & Lazarus, P. (2014). Regulation of UDP-glucuronosyltransferase 1A1 expression and activity by microRNA 491-3p. *J Pharmacol Exp Ther, 348*(3), 465-477. doi:10.1124/jpet.113.210658

Dluzen, D. F., Sutliff, A. K., Chen, G., Watson, C. J., Ishmael, F. T., & Lazarus, P. (2016). Regulation of UGT2B Expression and Activity by miR-216b-5p in Liver Cancer Cell Lines. *J Pharmacol Exp Ther, 359*(1), 182-193. doi:10.1124/jpet.116.235044

Fabian, M. R., Cieplak, M. K., Frank, F., Morita, M., Green, J., Srikumar, T., . . . Sonenberg, N. (2011). miRNA-mediated deadenylation is orchestrated by GW182 through two conserved motifs that interact with CCR4-NOT. *Nat Struct Mol Biol, 18*(11), 1211-1217. doi:10.1038/nsmb.2149

Fallon, J. K., Neubert, H., Hyland, R., Goosen, T. C., & Smith, P. C. (2013). Targeted quantitative proteomics for the analysis of 14 UGT1As and -2Bs in human liver using NanoUPLC-MS/MS with selected reaction monitoring. *J Proteome Res, 12*(10), 4402-4413. doi:10.1021/pr4004213

Gallagher, C. J., Muscat, J. E., Hicks, A. N., Zheng, Y., Dyer, A. M., Chase, G. A., . . . Lazarus, P. (2007). The UDP-glucuronosyltransferase 2B17 gene deletion polymorphism: sex-specific association with urinary 4-(methylnitrosamino)-1-(3-pyridyl)-1-butanol glucuronidation phenotype and risk for lung cancer. *Cancer Epidemiol Biomarkers Prev, 16*(4), 823-828.

Guo, G. X., Li, Q. Y., Ma, W. L., Shi, Z. H., & Ren, X. Q. (2015). MicroRNA-485-5p suppresses cell proliferation and invasion in hepatocellular carcinoma by targeting stanniocalcin 2. *Int J Clin Exp Pathol, 8*(10), 12292-12299.

Huang, R. S., Zheng, Y. L., Li, C., Ding, C., Xu, C., & Zhao, J. (2018). MicroRNA-485-5p suppresses growth and metastasis in non-small cell lung cancer cells by targeting IGF2BP2. *Life Sci, 199*, 104-111. doi:10.1016/j.lfs.2018.03.005

Innocenti, F., Iyer, L., Ramirez, J., Green, M. D., & Ratain, M. J. (2001). Epirubicin glucuronidation is catalyzed by human UDP-glucuronosyltransferase 2B7. *Drug Metab Dispos, 29*(5), 686-692.

Jones, N. R., & Lazarus, P. (2014). UGT2B gene expression analysis in multiple tobacco carcinogen-targeted tissues. *Drug Metab Dispos, 42*(4), 529-536. doi:10.1124/dmd.113.054718

Kang, M., Ren, M. P., Zhao, L., Li, C. P., & Deng, M. M. (2015). miR-485-5p acts as a negative regulator in gastric cancer progression by targeting flotillin-1. *Am J Transl Res, 7*(11), 2212-2222.

Kato, Y., Izukawa, T., Oda, S., Fukami, T., Finel, M., Yokoi, T., & Nakajima, M. (2013). Human UDP-glucuronosyltransferase (UGT) 2B10 in drug N-glucuronidation: substrate screening and comparison with UGT1A3 and UGT1A4. *Drug Metab Dispos, 41*(7), 1389-1397. doi:10.1124/dmd.113.051565

Lamba, V., Ghodke-Puranik, Y., Guan, W., & Lamba, J. K. (2014). Identification of suitable reference genes for hepatic microRNA quantitation. *BMC Res Notes, 7*, 129. doi:10.1186/1756-0500-7-129

Liu, J., Valencia-Sanchez, M. A., Hannon, G. J., & Parker, R. (2005). MicroRNA-dependent localization of targeted mRNAs to mammalian P-bodies. *Nat Cell Biol, 7*(7), 719-723. doi:10.1038/ncb1274

Lou, C., Xiao, M., Cheng, S., Lu, X., Jia, S., Ren, Y., & Li, Z. (2016). MiR-485-3p and miR-485-5p suppress breast cancer cell metastasis by inhibiting PGC-1alpha expression. *Cell Death Dis, 7*, e2159. doi:10.1038/cddis.2016.27

Lu, D., Xie, Q., & Wu, B. (2017). N-glucuronidation catalyzed by UGT1A4 and UGT2B10 in human liver microsomes: Assay optimization and substrate identification. *J Pharm Biomed Anal, 145*, 692-703. doi:10.1016/j.jpba.2017.07.037

Mackenzie, P. I., Bock, K. W., Burchell, B., Guillemette, C., Ikushiro, S., Iyanagi, T., . . . Nebert, D. W. (2005). Nomenclature update for the mammalian UDP glycosyltransferase (UGT) gene superfamily. *Pharmacogenet Genomics, 15*(10), 677-685.

Margaillan, G., Levesque, E., & Guillemette, C. (2016). Epigenetic regulation of steroid inactivating UDP-glucuronosyltransferases by microRNAs in prostate cancer. *J Steroid Biochem Mol Biol, 155*(Pt A), 85-93. doi:10.1016/j.jsbmb.2015.09.021

Nakamura, A., Nakajima, M., Yamanaka, H., Fujiwara, R., & Yokoi, T. (2008). Expression of UGT1A and UGT2B mRNA in human normal tissues and various cell lines. *Drug Metab Dispos, 36*(8), 1461-1464. doi:dmd.108.021428 [pii]

10.1124/dmd.108.021428

Ohno, S., & Nakajin, S. (2009). Determination of mRNA expression of human UDP-glucuronosyltransferases and application for localization in various human tissues by real-time reverse transcriptase-polymerase chain reaction. *Drug Metab Dispos, 37*(1), 32-40. doi:dmd.108.023598 [pii]

10.1124/dmd.108.023598

Papageorgiou, I., & Court, M. H. (2017). Identification and validation of the microRNA response elements in the 3'-untranslated region of the UDP glucuronosyltransferase (UGT) 2B7 and 2B15 genes by a functional genomics approach. *Biochem Pharmacol, 146*, 199-213. doi:10.1016/j.bcp.2017.09.013

Pfaffl, M. W. (2004). Quantification strategies in real-time PCR. In S. A. Bustin (Ed.), *A-Z of quantitative PCR* (pp. 87-112). La Jolla, CA International University Line

Shi, J., Wang, X., Lyu, L., Jiang, H., & Zhu, H. J. (2018). Comparison of protein expression between human livers and the hepatic cell lines HepG2, Hep3B, and Huh7 using SWATH and MRM-HR proteomics: Focusing on drug-metabolizing enzymes. *Drug Metab Pharmacokinet, 33*(2), 133-140. doi:10.1016/j.dmpk.2018.03.003

Stingl, J. C., Bartels, H., Viviani, R., Lehmann, M. L., & Brockmoller, J. (2014). Relevance of UDP-glucuronosyltransferase polymorphisms for drug dosing: A quantitative systematic review. *Pharmacol Ther, 141*(1), 92-116. doi:10.1016/j.pharmthera.2013.09.002

Sun, X., Liu, Y., Li, M., Wang, M., & Wang, Y. (2015). Involvement of miR-485-5p in hepatocellular carcinoma progression targeting EMMPRIN. *Biomed Pharmacother, 72*, 58-65. doi:10.1016/j.biopha.2015.04.008

Tatsumi, N., Tokumitsu, S., Nakano, M., Fukami, T., & Nakajima, M. (2018). miR-141-3p commonly regulates human UGT1A isoforms via different mechanisms. *Drug Metab Pharmacokinet, 33*(4), 203-210. doi:10.1016/j.dmpk.2018.05.002

Vandesompele, J., De Preter, K., Pattyn, F., Poppe, B., Van Roy, N., De Paepe, A., & Speleman, F. (2002). Accurate normalization of real-time quantitative RT-PCR data by geometric averaging of multiple internal control genes. *Genome Biol, 3*(7), RESEARCH0034.

Walsky, R. L., Bauman, J. N., Bourcier, K., Giddens, G., Lapham, K., Negahban, A., . . . Goosen, T. C. (2012). Optimized assays for human UDP-glucuronosyltransferase (UGT) activities: altered alamethicin concentration and utility to screen for UGT inhibitors. *Drug Metab Dispos, 40*(5), 1051-1065. doi:10.1124/dmd.111.043117

Wiener, D., Fang, J. L., Dossett, N., & Lazarus, P. (2004). Correlation between UDP-glucuronosyltransferase genotypes and 4-(methylnitrosamino)-1-(3-pyridyl)-1-butanone glucuronidation phenotype in human liver microsomes. *Cancer Res, 64*(3), 1190-1196.

Wijayakumara, D. D., Hu, D. G., Meech, R., McKinnon, R. A., & Mackenzie, P. I. (2015). Regulation of Human UGT2B15 and UGT2B17 by miR-376c in Prostate Cancer Cell Lines. *J Pharmacol Exp Ther, 354*(3), 417-425. doi:10.1124/jpet.115.226118

Wijayakumara, D. D., Mackenzie, P. I., McKinnon, R. A., Hu, D. G., & Meech, R. (2017). Regulation of UDP-Glucuronosyltransferases UGT2B4 and UGT2B7 by MicroRNAs in Liver Cancer Cells. *J Pharmacol Exp Ther, 361*(3), 386-397. doi:10.1124/jpet.116.239707

Zhang, X. N., Zhou, J., & Lu, X. J. (2018). The long noncoding RNA NEAT1 contributes to hepatocellular carcinoma development by sponging miR-485 and enhancing the expression of the STAT3. *J Cell Physiol, 233*(9), 6733-6741. doi:10.1002/jcp.26371

Molecular Pharmacology Fast Forward. Published on September 25, 2019 as DOI: 10.1124/mol.119.115881
This article has not been copyedited and formatted. The final version may differ from this version.

Footnotes

Funding for these studies were provided by the National Institutes of Health, National Institutes of Environmental Health Sciences (Grant R01-ES025460) to P. Lazarus, the National Institutes of Health, National Heart, Lung, and Blood Institute (Grant R01-HL126969) to H.-J. Zhu, and the Health Sciences and Services Authority of Spokane, WA [Grant WSU002292] to WSU College of Pharmacy and Pharmaceutical Sciences.

Reprint requests: Philip Lazarus, Ph.D., Department of Pharmaceutical Sciences, Washington State University College of Pharmacy, PO Box 1495, Spokane, WA, 99210
Email:phil.lazarus@wsu.edu

Molecular Pharmacology Fast Forward. Published on September 25, 2019 as DOI: 10.1124/mol.119.115881
This article has not been copyedited and formatted. The final version may differ from this version.

Figure Legends

Figure 1. *In silico* prediction and binding of miR-485-5p to UGT2B10. The miRNA prediction algorithm TargetScan database were used to identify miRNA binding candidates for five UGT2Bs: 2B4, 2B7, 2B10, 2B15 and 2B17 mRNAs. miR-485-5p was predicted to bind to the 3′ UTR of UGT2B10; two proposed binding sites for miR-485-5p to the 3' UTR of UGT2B7 are shown. Numbers listed correspond to the MRE locations 3' of the translational stop codon for the corresponding UGT.

Figure 2. Expression of UGTs 2B7, 2B10 and 2B15 versus miR-485-5p in human liver samples. Expression levels of miR-485-5p were quantified using qRT-PCR and normalized to the geometric mean of miR-152-3p and miR-23b-3p in the same samples. The Y-axis represents the natural log transformed values for miR-485-5p. The X-axis represents the ratio of UGTs 2B7, 2B10 or 2B15 to the BSA internal standard, transformed to the natural log value.

Figure 3. UGT2B 3′ UTR luciferase activity in the presence of miR-485-5p mimics. Panel A, the pGL3-UGT2B10 3′-UTR luciferase vector contains 1,086 nucleotides of the UGT2B10 3′ UTR including the MRE for miR-485-5p. The pGL3-UGT2B10 3' UTR MRE deletion vector contains a four nucleotide deletion within the potential miR-485-5p MRE seed sequence. The two columns on the left were performed using transfections of the luciferase vector containing the wild-type UGT2B10 3' UTR; the two columns on the

Molecular Pharmacology Fast Forward. Published on September 25, 2019 as DOI: 10.1124/mol.119.115881
This article has not been copyedited and formatted. The final version may differ from this version.

right were performed using the luciferase vector containing the UGT2B10 3' UTR with its seed sequence deletion mutation. Panel B, the pGL3-UGT2B7 3′-UTR luciferase vector contains 251 nucleotides of the UGT2B7 3' UTR including the MRE for each of the two predicted binding sites for miR-485-5p. The pGL3-UGT2B7 3' UTR MRE deletion vectors each contain a four nucleotide deletion within the potential miR-485-5p MRE seed sequence. The two columns on the left were performed using transfections of the luciferase vector containing the wild-type UGT2B7 3' UTR; the next six columns on the right were performed using the luciferase vector containing the UGT2B7 3' UTR with seed sequence deletion mutations at Site 1, Site 2, or both sites together, as indicated on the graph. Panel C, the pGL3-UGT2B15 3' UTR luciferase vector contains 467 nucleotides of the UGT2B15 3' UTR. Luciferase reporter vectors were co-transfected into HEK293 cells with the pRL-TK renilla control vector along with 100 nM of miR-485-5p mimic or scrambled miRNA control. Columns represent the mean ± S.D. of at least three independent experiments and are normalized to the scrambled miRNA-transfected control. * $P<0.05$; ** $P<0.01$, all compared to the referent scrambled control miRNA co-transfected with the luciferase vector containing the corresponding wild-type UGT2B 3' UTR.

Figure 4. Glucuronidation activity in the presence of miR-485-5p mimic. Panel A, UGT2B10 glucuronidation activity against nicotine in HuH-7 cells transfected with 100 nM miR-485-5p mimic or 100 nM of scrambled miRNA control in HuH-7 and Hep3B cells. Columns represent the mean ± S.E. of four independent experiments. Panel B, UGT2B7 glucuronidation activity against AZT in HuH-7 cells transfected with 100 nM

Molecular Pharmacology Fast Forward. Published on September 25, 2019 as DOI: 10.1124/mol.119.115881
This article has not been copyedited and formatted. The final version may differ from this version.

scrambled or miR-485-5p mimic. Columns represent the mean ± S.D. of six independent experiments. * P<0.05; ** P<0.01, ***P<0.001.

Molecular Pharmacology Fast Forward. Published on September 25, 2019 as DOI: 10.1124/mol.119.115881
This article has not been copyedited and formatted. The final version may differ from this version.

Table 1. Quantitative PCR data for miRNA in normal human liver specimens.[a]

microRNA	Mean	Std. deviation	Max. value	Min. value
miR-379-5p	0.6540	0.3377	1.7136	0.2418
miR-135a-5p	0.0290	0.0400	0.2792	0.0007
miR-590-5p	1.1699	0.7811	4.4453	0.2338
miR-216a-5p	0.0716	0.0505	0.2085	0.0127
miR-216b-5p	0.0215	0.0197	0.0934	0.0004
miR-146a-3p	0.0089	0.0061	0.0268	0.0022
miR-196a-5p	0.2286	0.8009	6.3672	0.0140
miR-485-5p	0.0031	0.0020	0.0111	0.0009

[a] miRNA expression levels were normalized using the method of Lamba et al. (2014).

Molecular Pharmacology Fast Forward. Published on September 25, 2019 as DOI: 10.1124/mol.119.115881
This article has not been copyedited and formatted. The final version may differ from this version.

Figure 1

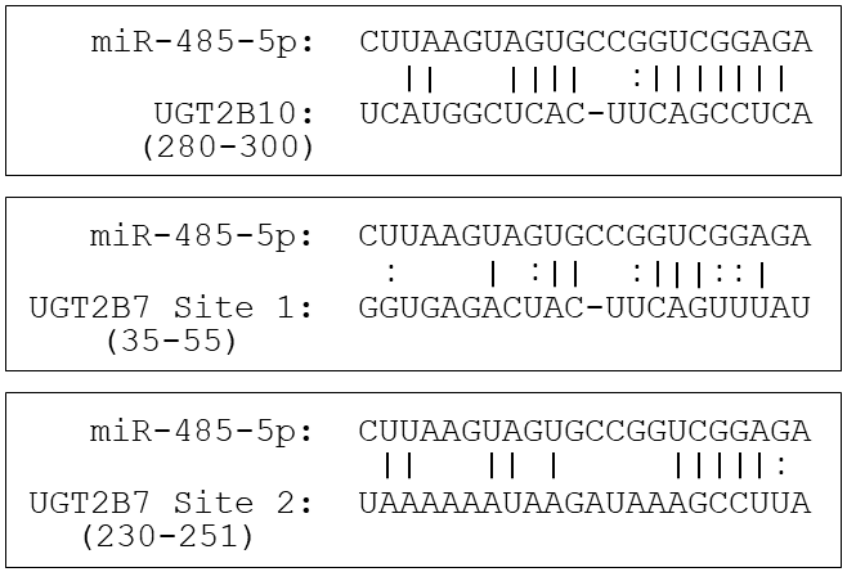

Molecular Pharmacology Fast Forward. Published on September 25, 2019 as DOI: 10.1124/mol.119.115881
This article has not been copyedited and formatted. The final version may differ from this version.

Figure 2

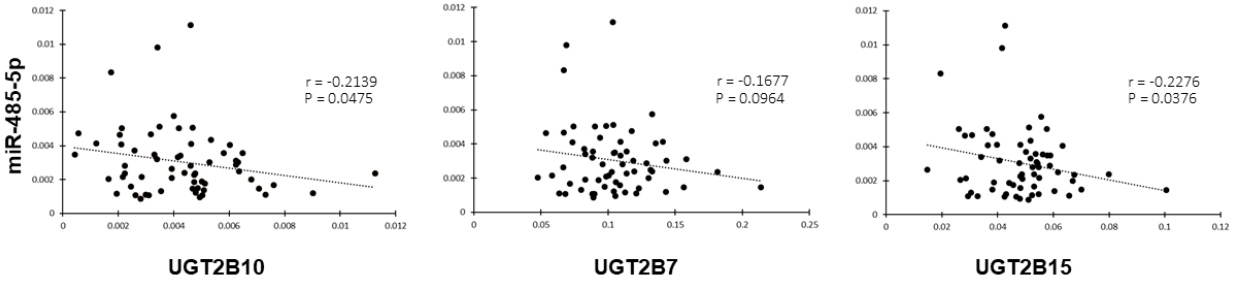

Molecular Pharmacology Fast Forward. Published on September 25, 2019 as DOI: 10.1124/mol.119.115881
This article has not been copyedited and formatted. The final version may differ from this version.

Figure 3

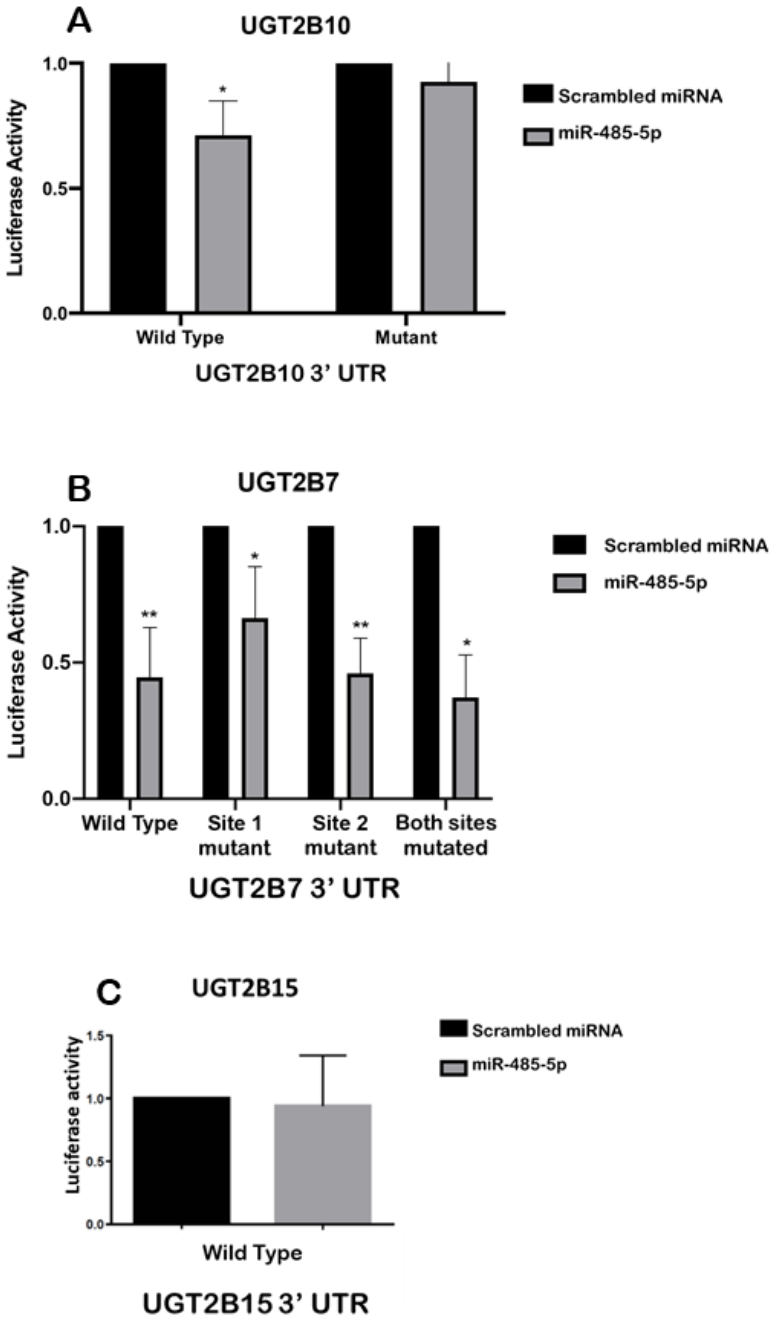

Molecular Pharmacology Fast Forward. Published on September 25, 2019 as DOI: 10.1124/mol.119.115881
This article has not been copyedited and formatted. The final version may differ from this version.

Figure 4